Solar cycle influences on the shape and location of the Earth's magnetopause

K. M. Raymer[1,*], S. M. Imber[1] and S. E. Milan[1]

*kmr18@leicester.ac.uk

[1]Dept. of Physics and Astronomy, University of Leicester, UK

1. Abstract

The location of the magnetopause is governed by a combination of internal magnetospheric and external solar wind parameters. While the dependence on upstream **solar wind dynamic pressure**, P_{dyn}, and direction of the interplanetary magnetic field (IMF) $\mathbf{B_z}$ component have been the subject of many studies, few have characterised the influence of internal parameters.

We employ an automated routine to identify magnetopause crossings made by the Geotail spacecraft over almost **two solar cycles**. A total of **8561 crossings** are found where upstream solar wind data are available.

To investigate how the magnetopause location changes with solar cycle, we first find out how it **varies with the upstream P_{dyn}**; the main driver of magnetopause motion. This is done by fitting the *Shue et al.* [1997] function to our dataset and allows us to predict where the magnetopause should be based on P_{dyn}. We then explore how its shape and location varies over a solar cycle and other parameters.

2. Magnetopause crossing detection

The automated routine identifies magnetopause crossings based on magnetic field and plasma measurements from the Geotail spacecraft.

It is applied to 20 years of data (1996 - 2015) and **8561 magnetopause crossings** are identified with corresponding upstream solar wind data from the OMNI dataset. Below are the complete set of crossing locations:

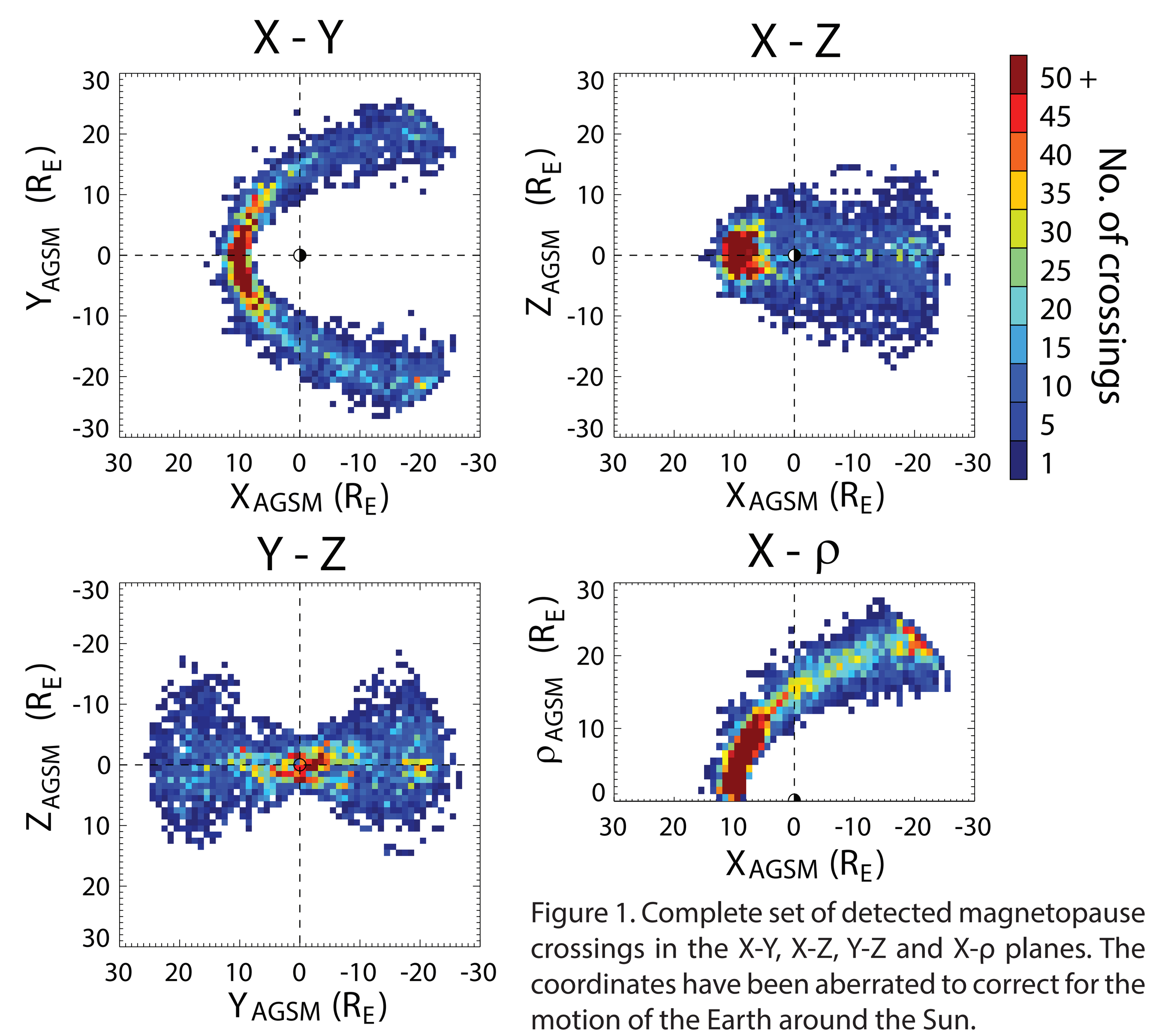

Figure 1. Complete set of detected magnetopause crossings in the X-Y, X-Z, Y-Z and X-ρ planes. The coordinates have been aberrated to correct for the motion of the Earth around the Sun.

There are more dayside crossings than nightside due to the orbital path of Geotail. Its orbit is mainly equatorial, and its apogee covers all magnetic local times in the course of a year.

3. Solar cycle dependence

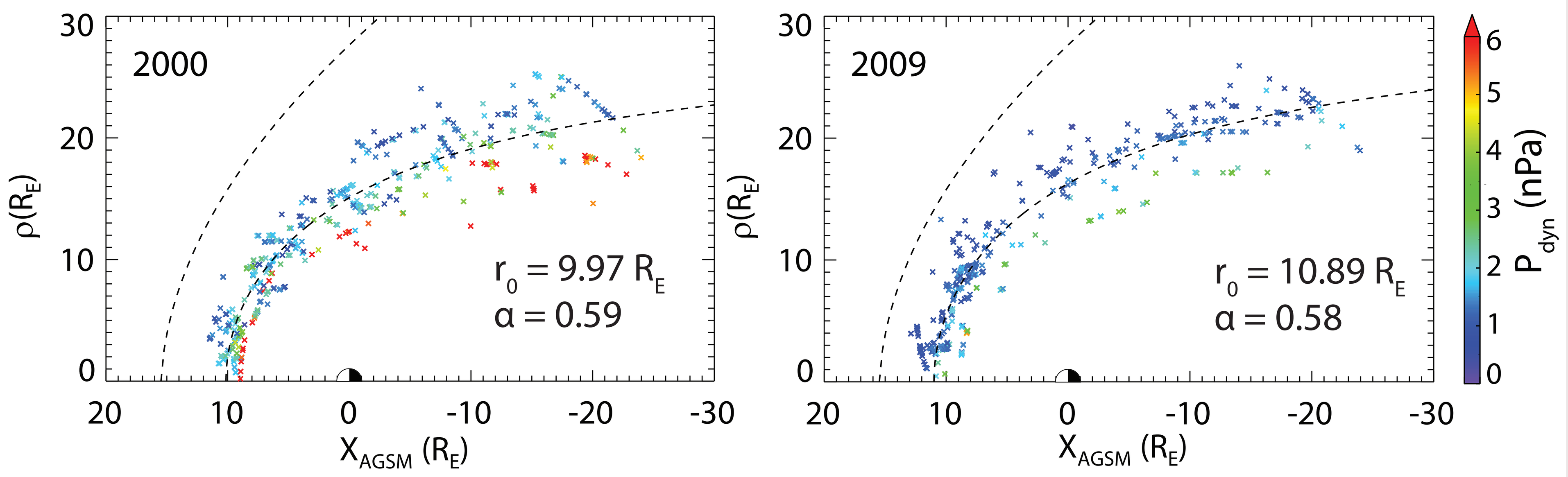

Figure 2. The above two plots show all of the crossings identified in 2000 and 2009 colour coded with solar wind dynamic pressure (from the OMNI dataset). Plotted on top are a model bow shock (*Peredo et al.*, 1995) and model magnetopause (*Shue et al.*, 1998) which are based on the average solar wind conditions for the crossings in each year.

At solar maximum we see higher solar wind dynamic pressures and the magnetopause is located closer to Earth. The solar minimum in 2009 was much deeper than previous solar minima. We see low dynamic pressures and an inflated magnetosphere.

4. Finding the dependence on solar wind dynamic pressure

The function defined by *Shue et al.* [1997] describes the shape and location of the magnetopause and is derived from in situ spacecraft data. It is given by $r = r_0\,(2/[1+\cos\theta])^{\alpha}$, where r_0 is the magnetopause standoff distance and α is the level of flaring in the magnetotail.

- We separate our crossings into 1 nPa P_{dyn} bins and fit the *Shue et al.* function to each set.
- r_0 and α are calculated as follows:

$$r_0 = 10.89\,P_{dyn}^{-1/8.6}$$

$$\alpha = 0.59 - 0.008\,P_{dyn}$$

- As solar wind pressure increases, the magnetopause standoff distance moves closer to the planet and the magnetotail compresses. This can be clearly seen at the two solar maxima.
- During solar minimum, the magnetopause inflates.
- It is clear however, there are other factors causing magnetopause motion.

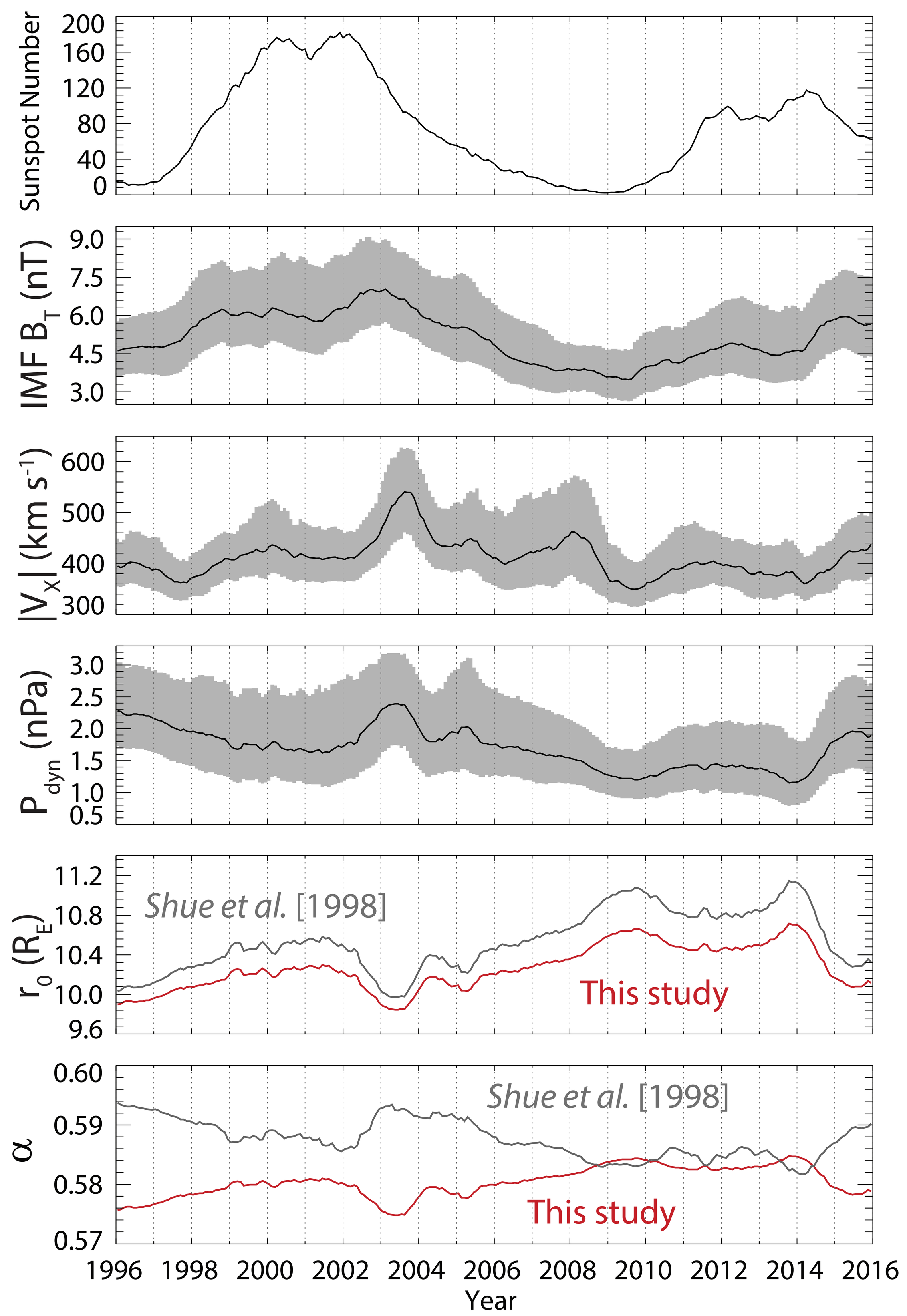

Figure 3. 12 month sliding average sunspot numbers are calculated from the WDC-SILSO database, and 12 month sliding average B_T, $|V_X|$ and P_{dyn} are calculated from the OMNI dataset. Red (grey) indicates results from this study (*Shue et al.* [1998] study).

5. Dependence on other parameters

The predicted magnetopause location is calculated for each crossing, based on P_{dyn}. The distance between the actual crossing location and this expected location is presented below in the Figures 4a-d, along with the corresponding IMF B_z, the dayside reconnection rate, φ_D, the SYM-H ring current index, and the open flux content (measured by auroral images), respectively. The crosses and error bars indicate the median and interquartile ranges for each row.

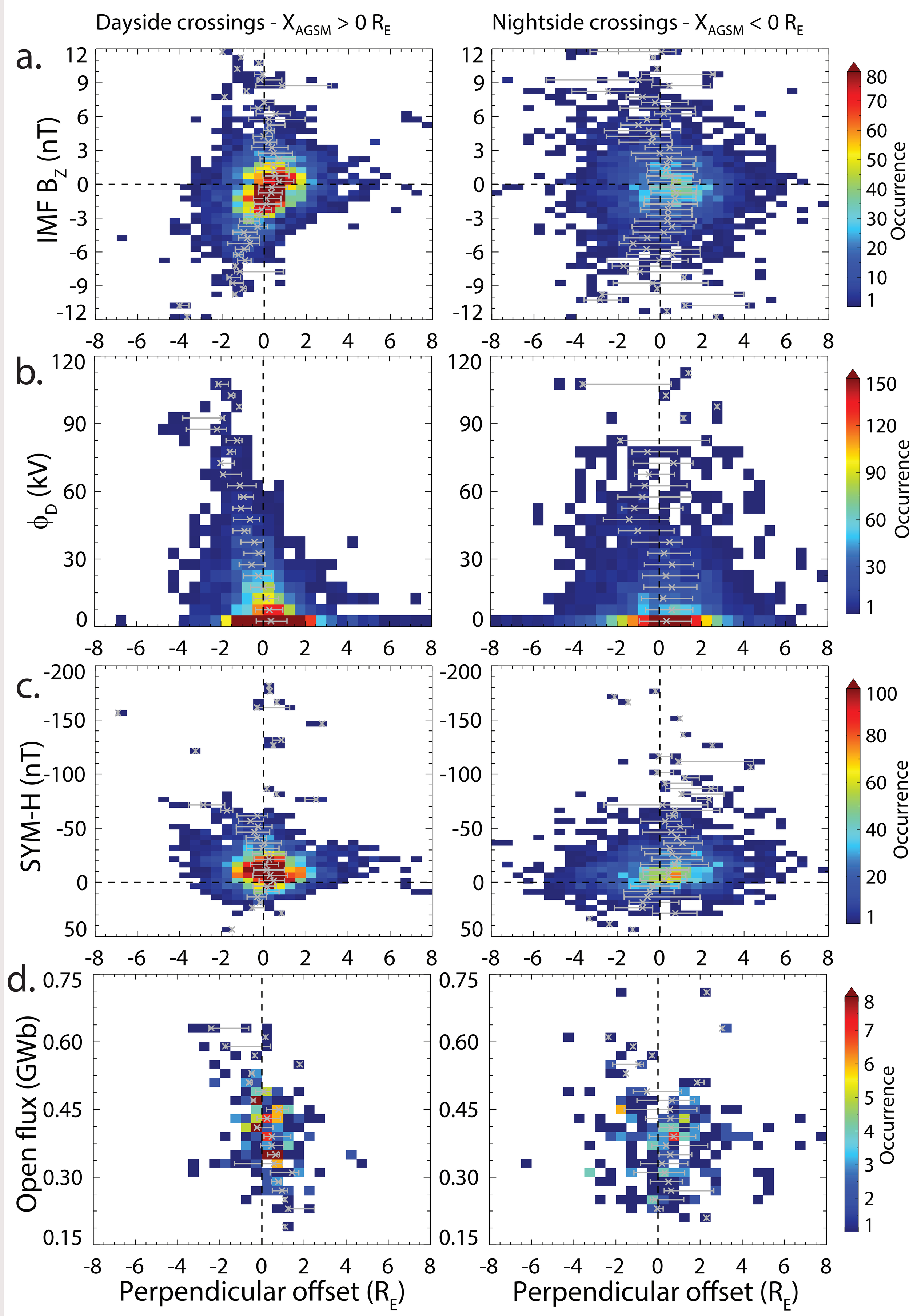

Figure 4a. We observe a compression of the dayside magnetopause when the IMF B_z is directed southwards. The nightside magnetopause is much more varied in comparison.

Figure 4b. As the dayside reconnection rate, φ_D, increases, i.e. more magnetic flux is being eroded, the dayside magnetopause moves closer to the planet.

Figure 4c. During disturbed times when SYM-H decreases, we see a slight compression of the dayside magnetopause and an inflation of the nightside magnetopause. We believe this can be attributed to an enhanced ring current.

Figure 4d. The IMAGE satellite was in operation for a much shorter period than Geotail and hence we have fewer crossings. When there is more open flux in the magnetosphere, the dayside magnetopause is eroded. The nightside magnetopause, however, is expanded.

6. Conclusions

- P_{dyn} plays a vital role in ordering the magnetopause shape and location. This study shows that during periods of strong (weak) P_{dyn}, the magnetopause is compressed (inflated) at **both the dayside and nightside**, unlike previous studies.
- The erosion of the dayside magnetopause during periods of southward IMF B_z is clearly seen in both Figures 4a and 4b. In comparison, the nightside magnetopause is much more malleable.
- During geomagnetic storms the ring current becomes enhanced and the perturbed magnetic field outside the ring current acts to inflate the magnetopause. This is visible in Figure 4c.
- Figure 4d shows that as the amount of open flux in the magnetosphere increases, the dayside magnetopause erodes and the nightside magnetopause expands.

References:
Case, N. A., and J. A. Wild (2013), *J. Geophys. Res. Space Physics*, *118*, 6127-6135;
Ivchenko, N. V., et al. (2000), *Geophys. Res. Lett.*, *27*(18), 2881-2884;
Milan, S. E., et al. (2012), *J. Geophys. Res.*, *117*, A03226;
Shue, J.-H., et al. (1997), *J. Geophys. Res.*, 102, 9497–9511;
Shue, J.-H., et al. (1998), *J. Geophys. Res.*, *103*(A8), 17,691–17,700;
Peredo, M., et al. (1995), *J. Geophys. Res.*, *100*(A5), 7906-7916.

Acknowledgements: K. M. R. was supported by a STFC studentship. All Geotail data are from the Institute of Space and Astronautical Science/Japan Aerospace Exploration Agency (ISAS/JAXA). The magnetic field and ion moment data are available from the Data Archives and Transmission System (DARTS). The authors would like to thank the PI of the Magnetic Field Experiment T. Nagai for his help in accessing recent data. We gratefully acknowledge the NASA/GSFC Space Physics Data Facility's OMNIWeb service, as well as S. Mende for access to the IMAGE data.